Synthesis and Characterization of Novel Methacrylate Monomers Having Pendant Oxime Esters and Their Copolymerization with Styrene

M. Arif Koroglu[a]; Ibrahim Erol[a]; Elif Korcan[b]; Muhsin Konuk[b]

[a] Faculty of Science and Arts, Department of Chemistry, Afyon Kocatepe University, Afyonkarahisar, Turkey [b] Faculty of Science and Arts, Department of Biology, Afyon Kocatepe University, Afyonkarahisar, Turkey

PLEASE SCROLL DOWN FOR ARTICLE

Synthesis and Characterization of Novel Methacrylate Monomers Having Pendant Oxime Esters and Their Copolymerization with Styrene

M. ARIF KOROGLU,[1] IBRAHIM EROL,[1] ELIF KORCAN,[2] and MUHSIN KONUK[2]

[1]*Faculty of Science and Arts, Department of Chemistry, Afyon Kocatepe University, Afyonkarahisar, Turkey*
[2]*Faculty of Science and Arts, Department of Biology, Afyon Kocatepe University, Afyonkarahisar, Turkey*
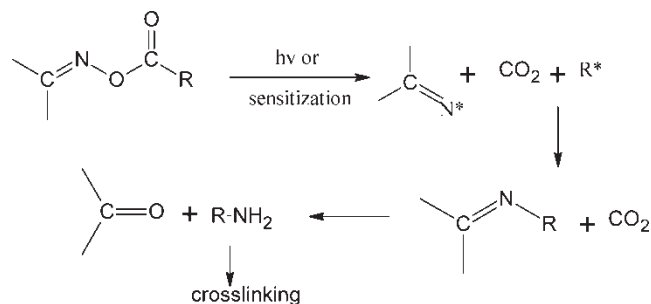
New methacrylate monomers, 2-{[(diphenylmethylene)amino]oxy}-2-oxoethyl methacrylate (DPOMA) and 2-{[(1-phenylethylidene)amino]oxy}-2-oxoethyl methacrylate (MMOMA) were prepared by reaction of sodium methacrylate with diphenylmethanone *O*-(2-chloroacetyl) oxime and 1-phenylethanone *O*-(2-chloroacetyl) oxime, respectively. They were obtained from a reaction of chloroacetyl chloride with benzophenone oxime or acetophenone oxime. The free-radical-initiated copolymerization of (DPOMA) and (MMOMA) with styrene (St) were carried out in 1,4-dioxane solution at 65°C using 2,2-azobisisobutyronitrile (AIBN) as an initiator with different monomer-to-monomer ratios in the feed. The monomers and copolymers were characterized by FTIR, ^{1}H- and ^{13}C-NMR spectral studies. The copolymer compositions were evaluated by nitrogen content in polymers. The reactivity ratios of the monomers were determined by the application of Fineman–Ross and Kelen–Tüdös methods. The molecular weights ($\bar{M}_w$ and $\bar{M}_n$) and polydispersity index of the polymers were determined by using gel permeation chromatography. Thermogravimetric analysis of the polymers reveals that the thermal stability of the copolymers increases with an increase in the mole fraction of St in the copolymers. The activation energies of the thermal degradation of the polymers were calculated with the MHRK method. Glass transition temperatures of the copolymers were found to decrease with an increase in the mole fraction of DPOMA or MMOMA in the copolymers. The antibacterial and antifungal effects of the monomers and polymers were also investigated on various bacteria and fungi. The photochemical properties of the polymers were investigated by UV and FTIR spectra.

Keywords: oxime esters; methacrylate; monomer reactivity ratios; biological activity; thermal stability; activation energies

1 Introduction

Nowadays, the synthesis of functional monomers and their polymers and use in the synthesis of new functional polymers have attracted considerable interest. Methacrylic polymers find extensive applications in fiber optics, metal complexes, polymeric reagents, and polymeric supports (1–5). Recent investigations report the use of oxime esters as irreversible acyl transfer agents where the leaving group, the oxime does not participate in the back reaction (6). This methodology has been elegantly utilized for the preparation of chiral polymers (7), regioselective acylation of nucleosides and to obtain various nucleoside derivatives of medicinal significance (8). In a previous report (9), methacrylate containing oxime ester moieties used as irreversible acyl transfer

agents. Athawale and coworker synthesized geranyl methacrylate and (±) mentyl methacrylate by a transesterification reaction using 2,3-butane dione mono-oxime methacrylate as acylating agents (10, 11). *O*-acyloximes can be used as photobase generators and they have been proved to be quite efficient (12–17). In the case of phenyl acetyloximes, a schematic process for amine production can be given as:

For carbomyl derivatives, direct hydrogen abstraction from the substrate to R leads to the formation of amine without

Address correspondence to: Ibrahim Erol, Faculty of Science and Arts, Department of Chemistry, Afyon Kocatepe University, Afyonkarahisar, Turkey. Tel.: + 90 272 2281311; Fax: +90 272 2281235; E-mail: iberol@hotmail.com or ierol@aku.edu.tr

requirement of water (18). In previous studies, photolysis of oxime esters based on antraquinone were discussed as photo induced DNA cleaving agents for single and double strand scissions (19–21). It is well known from the literature that the compounds containing oxime esters moiety have a strong ability to form metal complexes and exhibit a wide range of biological activities (22–25).

Reactivity ratios are among the most important parameters for the composition equation of copolymers, which can offer information such as relative reactivity of monomer pairs and estimate the copolymer composition. Knowledge of the copolymer composition is an important step in the evaluation of its utility. Copolymer composition and its distribution are dependent on the reactivity ratios. The most common mathematical model of copolymerization is based on finding the relationship between the composition of copolymers and the composition of the monomer feed in which the monomer reactivity ratios are the parameters to be determined (26, 27). The calculation of the monomer reactivity ratios requires the mathematical treatment of experimental data on the compositions of copolymers and monomer feed mixtures. The microstructure and composition of copolymers are important factors in copolymer properties. For the design of new copolymer materials, prediction of microstructure and composition from copolymerization kinetics, via monomer reactivity ratios, is of primary importance. The accurate determination of copolymer composition and estimation of monomer reactivity ratios are significant for tailor-made copolymers with desirable physical and chemical properties and in evaluating the specific end application of copolymers. The main aim in commercial copolymerization is to achieve as specific a composition distribution as possible. Knowledge about the monomer reactivity ratios would help in achieving this. Monomer reactivity ratios were determined by a number of linearization methods (28, 29). Thermogravimetric analysis (TGA) has been widely used to investigate the decomposition characteristics of many materials. Some methods have already been established to evaluate the kinetic parameters from thermogravimetric data (30–32).

We report here the preparation of new methacrylate esters with pendant oxime esters moieties based on acetophenone and benzophenone, as well as their free radical copolymerization behavior. In addition, these monomers were copolymerized with styrene (St) and the monomer reactivity ratios calculated using Kelen-Tüdos and Fineman-Ross methods. The biological activities and activation energies of the copolymers were also obtained. The photochemical properties of polymers were investigated by Ultraviolet spectrometer.

2   Experimental

2.1   Materials

Acetophenone, benzophenone, chloracetylchloride, hydroxylamino hydrochloride and sodium hydroxide (Merck), sodium

methacrylate, 1,4-dioxane, potassium carbonate, acetonitrile, anhydrous magnesium sulphate (Aldrich) were used as received. 2,2′-Azobisisobutyronitrile was recrystallized from chloroform-methanol. Bactopeptone and glucose was obtained from difco. All the other chemicals were analytical grade and used without any further purification. Styrene (St) was freed from the inhibitor by washing with 5% NaOH solution followed by distilled water, and after drying over anhydrous sodium sulphate it was distilled under vacuum.

2.2   Characterization Techniques

IR spectra were measured on a Perkin-Elmer Spectrum BX FT-IR spectrometer. ^{1}H- and ^{13}C-NMR spectra were recorded in CDCl$_3$ with tetramethylsilane as the internal standard using on Bruker GmbH DPX-400 400 MHz spectrometer. Thermal data were obtained by using a Perkin-Elmer DSC instrument and TGA thermobalance in N$_2$ atmosphere. Molecular weight; ($\bar{M}_w$ and $\bar{M}_n$) of the polymers were determined by e waters 410 gel permeation chromatography equipped with a differential refractive index detector and calibrated with polystyrene standards. Elemental analyses were carried out by a LECO CHNSO-932 auto microanalyzer.

2.3   Synthesis Diphenylmethanone O-(2-chloroacetyl) Oxime

Synthesis of diphenylmethanone *O*-(2-chloroacetyl) oxime was as follows: Benzophenone oxime (33) (1 mol) and K$_2$CO$_3$ (0.1 mol) was dissolved in 20 ml of anhydrous CH$_2$Cl$_2$ at 0°C, and then chloracetylchloride (1.1 mol) were added dropwise to the solution. The reaction mixture was stirred at room temperature for 12 h. (Scheme 1). The organic layer was washed several times with diethylether
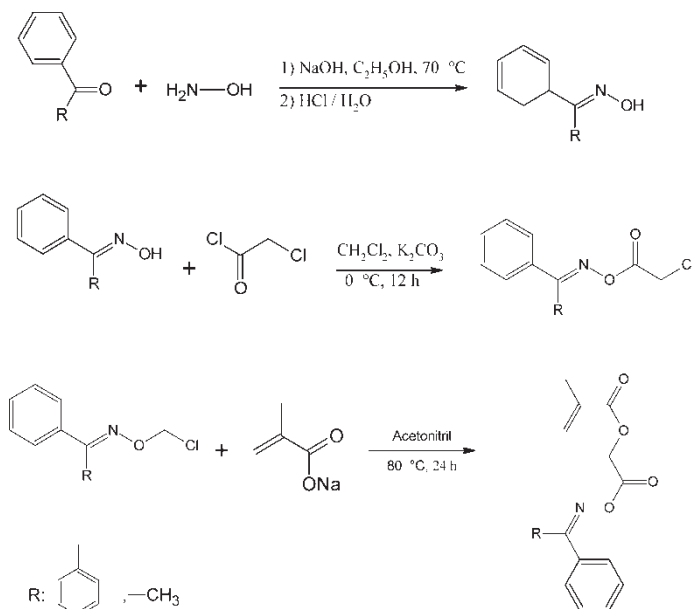
Sch. 1.   Synthesis of the monomers.

and dried over MgSO$_4$. After removing diethylether, diphenylmethanone *O*-(2-chloroacetyl) oxime was crystallized from ethanol. The yield was: 80%. Elemental analysis (%): C = 65.72 (Found), 65.82 (Calcd) H = 4.33 (Found), 4.42 (Calcd) N = 5.01 (Found) 5.12 (Calcd).

IR (neat), cm^{-1}: 1780 (C=O oxime ester carbonyl), 1610 (aromatic C=C), 1567 (C=N-), 727 (C-Cl; no O-H absorption).

2.4 Synthesis of 1-Phenylethanone O-(2-chloroacetyl) Oxime

Synthesis of 1-phenylethanone *O*-(2-chloroacetyl) oxime was similarly synthesized, expect that the product was crystallized rather than distilled. The yield was: 80%. Elemental analysis (%): C = 56.60 (Found), 56.75 (Calcd) H = 4.63 (found), 4.76 (Calcd.) N = 6.54 (Found) 6.62 (calcd.).

IR (neat), cm^{-1}: 1790 (C=O for oxime ester carbonyl), 1605 (aromatic C=C), 1570 (C=N-), 735 (C=Cl; no O-H absorption).

2.5 Monomer Synthesis

The reactions paths are shown in Scheme 1. Diphenylmethanone *O*-(2-chloroacetyl) oxime (1 mol), and sodium methacrylate (1.1 mol) were stirred in 50 ml acetonitrile at 75°C in a reflux condenser for 24 h in the presence of 100 ppm hydroquinone as inhibitor. Then the solution was cooled to room temperature and neutralized with a 5% KOH solution. The organic layer was washed several times with water and the water layer was washed with diethylether a few times. The acetonitrile layer and diethylether layer were collected and dried over anhydrous MgSO$_4$ overnight. Acetonitrile and diethylether were evaporated. The organic layers were collected and the residue was crystallized from ethanol.

Elemental analysis (%): C = 70.49 (Found), 70.58 (Calcd) H = 5.18 (Found), 5.30 (Calcd) N = 4.24 (Found) 4.33 (Calcd). IR (KBr), cm^{-1}: 1780, 1724 (oxime ester and methacrylic carbonyl), 1630 (CH$_2$=C-), 1600 (C=C), 1570 (C=N). ^{1}H-NMR (δ, ppm from TMS in CDCl$_3$): 7.2–7.7 (aromatic protons, 10H); 5.6 (CH$_2$=, 1H); 6.2 (CH$_2$=, 1H); 4.8 (-OCH$_2$-, 2H); 2.1 (CH$_3$-, 3H). ^{13}C-NMR (δ, ppm from TMS in CDCl$_3$): 169.0 and 172.0 (C=O of esters); 133.0 (=C); 124.1 (CH$_2$=); 122.1–137.8 (aromatic carbons); 65.0 (-OCH$_2$-); 21.5 (CH$_3$).

The monomer of 2-{[(1-phenylethylidene) amino]oxy}-2-oxoethyl methacrylate (MMOMA) was similarly synthesized.

Elemental analysis (%): C = 65.72 (Found), 64.36 (Calcd.) H = 5.68 (Found), 5.79 (Calcd.). Nequals; 5.24 (Found) 5.36 (Calcd). IR (neat), cm^{-1}: 1790, 1724 (oxime ester and methacrylic carbonyl), 1630 (CH$_2$=C-), 1600 (C=C), 1573 (C=N). ^{1}H-NMR (δ, ppm from TMS in CDCl$_3$): 7.2–7.8 (phenyl ring protons, 5H); 5.6 (CH$_2$=, 1H); 6.3 (CH$_2$=, 1H); 5.0 (-OCH$_2$-, 2H); 2.3 (-N=CCH$_3$-, 3H); 1.9 (CH$_3$-3H). ^{13}C-NMR (δ, ppm from TMS in CDCl$_3$): 164.0 and 167 (C=O of esters); 133.0 (=C); 124.1 (CH$_2$=);

127–138 (phenyl carbons); 66.0 (-OCH$_2$-); 16 (-N=CCH$_3$-); 13 (CH$_3$).

2.6 Polymerization of the Monomers

Polymerization of (DPOMA) and (MMOMA) was carried out in glass ampoules under N$_2$ atmosphere in 1,4-dioxane solution with AIBN (1% based on the total weight of monomers) as an initiator. The reacting components were degassed by threefold freeze-thawing cycles and then immersed in oil bath at 65°C for a given reaction time. The polymers were separated by precipitation in ethanol and reprecipitated from dichloromethane solution. The polymers were finally dried under vacuum to constant weight at room temperature and kept in a dessicators under vacuum until use.

2.7 Copolymerization

Copolymerizations of St with (DPOMA) and (MMOMA) using different proportions of (St) were carried out in glass ampoules under N$_2$ atmosphere in 1,4-dioxane solution with AIBN (1%, based on the total weight of monomers) as an initiator. The reacting components were degassed by threefold freeze-thawing cycle and then immersed in a oil bath at 65 ± 0.1°C for a given reaction time. The reaction time was selected to give conversions less than 10% to satisfy the differential copolymerization equation. After the desired time the copolymers were separated by precipitation in ethanol and reprecipitated from CH$_2$Cl$_2$ solution. The polymers, purified by reprecipitation to avoid the formation of homopolymers. The polymers were finally dried over vacuum at 45°C to constant weight. The amounts of monomeric units in the copolymers were determined by elemental analysis. The results are presented in Table 1.

3 Results and Discussion

As shown in Scheme 1, the preparation of new methacrylate esters having pendant oxime esters moieties monomers were synthesized from diphenylmethanone *O*-(2-chloroacetyl) Solvent: 1,4 dioxane, temperature: 65 ± 1°C, initiator: AIBN(1% weight of monomers), non-solvent: ethanol oxime or 1-phenylethanone *O*-(2-chloroacetyl) oxime with sodium methacrylate, according to the usual method (34). The yields of the reactions in Scheme 1 are of medium quantity (70–80%). The structures of DPOMA and MMOMA were identified by elemental analysis, IR and NMR spectroscopy and the results were in good agreement with the structure of the compounds.

The free radical homopolymerization of the monomers was performed at 65°C in a 1,4-dioxane solution with 2,2-azobisisobutyronitrile (AIBN) as an initiator (Scheme 2).

Table 1. Copolymer composition data and molecular weight

System	M_2a	Conv. (%)	N^b(%)	$M_2{}^c$	$\bar{M}_w \times 10^4$	$\bar{M}_n \times 10^4$	$\bar{M}_w/\bar{M}_n$
Poly(MMOMA-co-St)							
1	0.20	9.40	4.65	0.28	4.52	2.87	1.57
2	0.35	8.50	4.21	0.41	4.48	2.37	1.88
3	0.50	8.00	3.92	0.48	5.43	3.12	1.74
4	0.65	8.65	3.63	0.55	5.14	2.82	1.82
5	0.80	9.60	2.86	0.69	3.96	2.20	1.80
6	0.90	9.50	2.14	0.79	7.12	4.00	1.78
Poly(MMOMA)					4.34	3.27	1.32
Poly(DPOMA-co-St)							
1	0.20	7.50	3.89	0.26	6.65	3.88	1.71
2	0.35	7.69	3.43	0.45	5.40	2.93	1.84
3	0.50	9.60	3.36	0.47	5.36	3.40	1.57
4	0.65	7.42	2.95	0.59	4.42	2.83	1.56
5	0.80	6.80	2.51	0.69	4.03	2.59	1.55
6	0.90	8.50	1.74	0.82	8.20	4.95	1.65
Poly(DPOMA)					4.82	2.94	1.63

[a]The mol fraction St in the feed.
[b]Determined by elemental analyses.
[c]The mol fraction St in the copolymer.

3.1 Structural Characterization of the Monomers and their Homopolymers

The FT-IR spectra of the MMOMA monomer and its polymer poly (MMOMA) are shown in Figure 1. The IR spectrum of the polymers showed some characteristic absorption peaks at 1741 cm^{-1} (ester carbonyl stretching) 1790 cm^{-1} (oxime ester carbonyl stretching), 1565 cm^{-1} (C=N). During the polymerization of the monomers, the IR band at 1630 cm^{-1} (C=C) disappearance and ester carbonyl stretching for polymers shifted to about 1740 cm^{-1}, whereas that of oxime ester carbonyl appeared at about 1795 cm^{-1}. The main evidence of the polymer is certainly the disappearance of some characteristic signals of the double bond in the spectra, and this fact was effectively observed in our case. Thus, two bands vanished in the IR spectrum: the absorption band at 923 cm^{-1} assigned to the C-H bending of geminal =CH$_2$ and the stretching vibration band of C=C at 1600 cm^{-1}. The ^{1}H-NMR spectrum of the DPOMA monomer is presented in Figure 2. The ^{1}H NMR spectra of the both monomers have the characteristic peaks of the monomeric units. The ^{1}H and ^{13}C-NMR spectra of the poly (MMOMA) are shown in Figure 3 and are in good agreement with the structure. From ^{1}H-NMR spectroscopy the formation of the polymer is also clearly evident from the vanishing of two singlets at 5.6 and 6.2 ppm of the vinyl protons and the appearance of the broad signal at 1.5 and 2.2 ppm assigned to an aliphatic -CH$_2$- group. In the proton decoupled ^{13}C-NMR spectrum of poly (MMOMA), chemical shift assignments were made from the off-resonance decoupled spectra of the polymer. Resonance signals at 168 ppm correspond to ester group present in the pendant oxime group in polymer. The ester carbonyl in the pendant methacrylate

resonance is observed at 165 ppm. The signal due to carbon of the aromatic ring attached to the C=N group shifts towards downfield and is observed at 137 ppm. The other aromatic carbons are observed at 125–135 ppm. The methylenoxy group flanked between the carbonyl group and ester group show signals at 60 ppm. The α-methyl group of polymer shows resonance signals at 14 ppm.

3.2 Characterization of the Copolymers

The constituent monomeric units of the copolymer are shown in Scheme 3. The FT-IR spectra of the DPOMA-St copolymers (Figure 4) show characteristic bands at 1785, 1740 cm^{-1} (oxime ester and, methacrylic ester carbonyl), 1567 cm^{-1} (-C=N), 3100–3000 cm^{-1} and 1608 cm^{-1} (phenyl). ^{1}H-NMR spectra show broad peaks at 7.0–7.9 ppm (phenyl
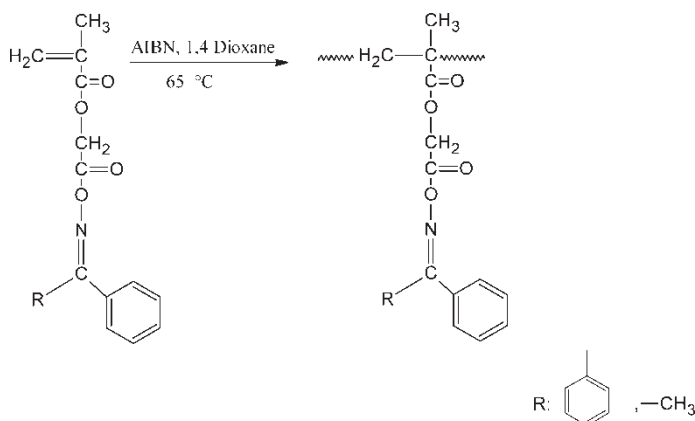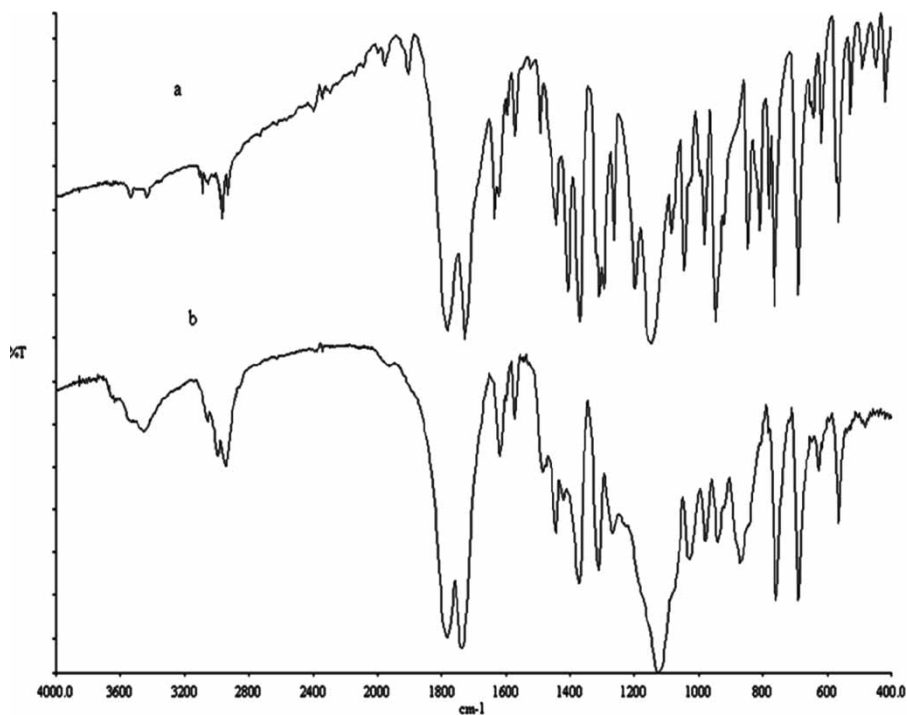

Sch. 2. Synthesis of the homopolymers.

Fig. 1. FT-IR spectra of MMOMA monomer (a) and it is polymer (b).

protons of two monomeric units), 4.6 ppm (-OCH$_2$ protons), 0.6–2.2 ppm (other aliphatic protons including those in the backbone). ^{13}C-NMR peak assigments of this copolymer are 63 ppm (-OCH$_2$ carbons), 124–135 ppm (Aromatic ring carbons) and, 165 and 167 ppm (oxime ester and, methacrylic ester carbonyl).

Although the FT-IR spectra of the MMOMA-St copolymers show characteristic bands at 1783, 1739 cm^{-1} (oxime and, methacrylic ester carbonyl), 1573 cm^{-1} (-C≡N), 3100–3000 cm^{-1} and 1610 cm^{-1} (phenyl). The ^{1}H-NMR spectrum of poly(MMOMA-co-St) (Figure 5) is consistent with its chemical structure. Multiplet resonance absorptions at 7.0–7.9 ppm are due to the aromatic protons of MMOMA and St units. The signals at 4.8 ppm are due to -OCH$_2$ protons. The backbone methylene protons of the two comonomer units are observed between 1.8–2.2 ppm. ^{13}C-NMR spectrum of MMOMA-St copolymer the resonance signals at 167 and 165 ppm are due to the oxime ester and methacrylic ester carbonyl carbons, respectively. The group of signals at 127–135 ppm arises from aromatic carbons in the two monomeric units. The signals at 67 ppm are due to the -OCH$_2$ carbons of MMOMA unit. The backbone methylene carbons of two comonomer units are observed at 47 ppm. The signal at 18 ppm corresponds to the α-methyl carbons of MMOMA unit.

3.3 UV Spectra of the Polymers

A solution of homo and copolymers in DMSO was cast onto a quartz glass plate with a spin coater and then was annealed for 30 min at 40°C. The thin film (0.8–1 μm) was irradiated with

a fixed energy of light from a Spex Fluorolog 2 with a 450-W xenon lamp. Figure 6 compares the absorption spectra of the polymers and the following includes the absorption characteristics in the UV spectra. The UV spectra of the polymers show an absorption maxima at 255 nm for poly(DPOMA), 250 nm for poly(MMOMA), and about 247 nm for copolymers due to the π-π^* transition of C≡C (phenyl) and C≡N of the pendant oxime ester group chromophore present in the polymer unit. The first observation to discuss is that the

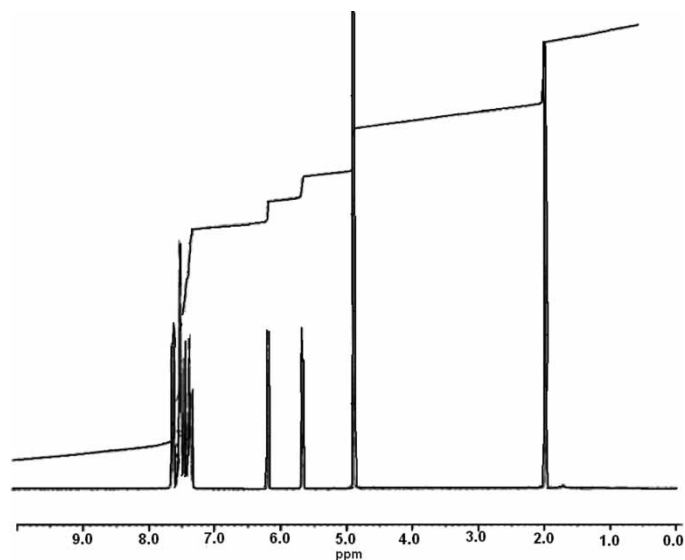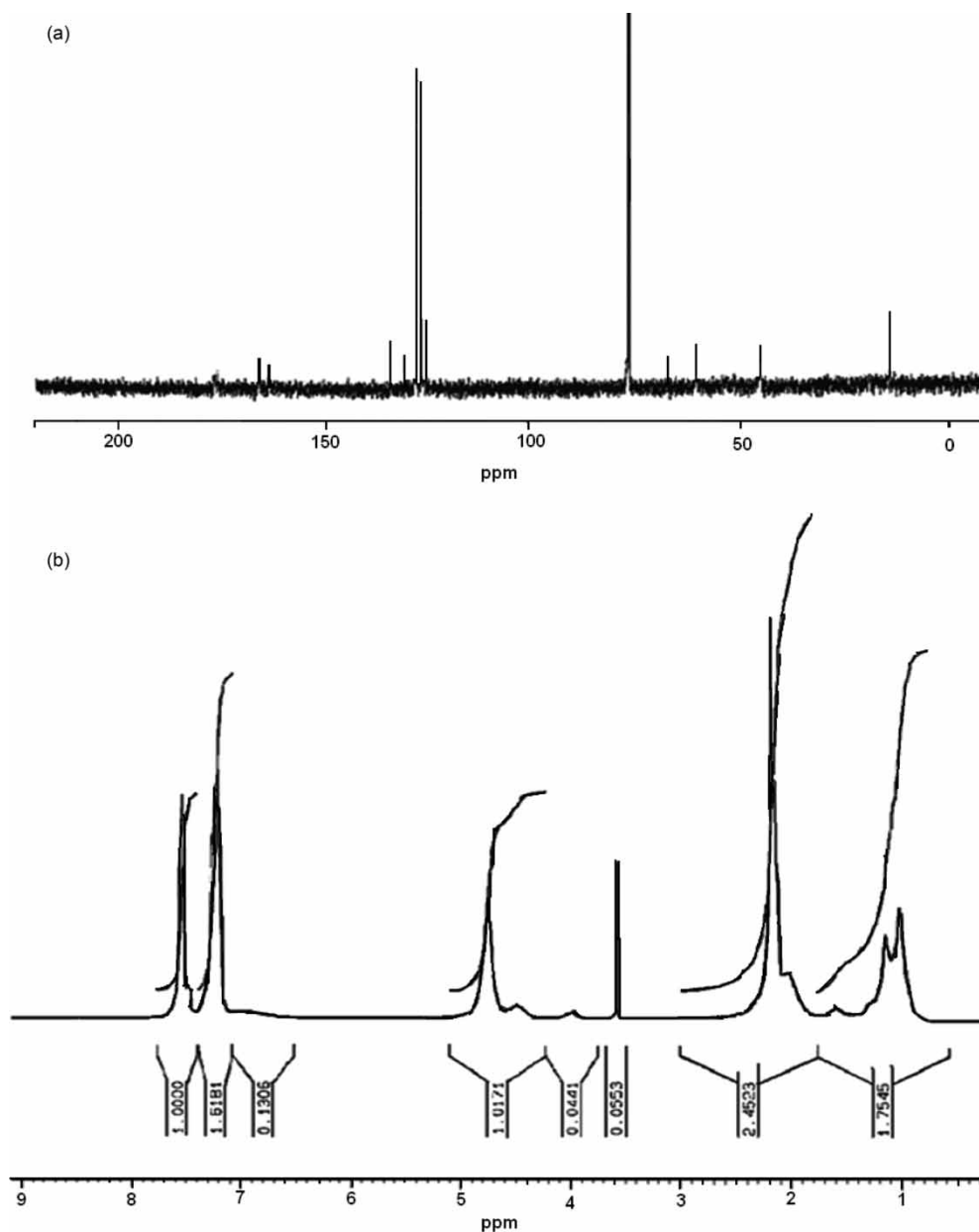**Fig. 2.** ^{1}H-NMR spectrum of DPOMA monomer.

Fig. 3. a) ^{1}H-NMR and b) ^{13}C-NMR spectra of poly(MMOMA).

fluorescence behavior for the poly (DPOMA) is different from that of the others. So this specific absorption spectrum of poly (DPOMA) suggests that energy states of chromophere substituted by two phenyl group differ somewhat from those of other chromophores. In fact, we had anticipated that the chromophore interactions in the present polymers would have been suppressed between the C=N groups attached in the vicinity of each chromophere group such as ester. It can be seen that the absorption properties are only slightly by the ester group. This is attributed to a $S_0 \rightarrow S_1$ transition localized on the oxime moiety. Due to their structural analogy and the presence of electron lone pair on the heteroatom, ketones were often compared with the corresponding oximes (35), the

question being the nature of the electronic transitions. The transition observed for the present oxime ester polymers are of π-π^* nature and the presence of a lone pair on the nitrogen atom do not lead to any observable n-π^* transition. Representative spectral change in UV absorption for films of poly (MMOMA) caused by the photoreaction upon irradiation with light 366 nm is presented in Figure 7. The absorption band at the longest wavelength decreased gradually with the increase of a new absorption band at around 200 nm. In addition, although all of the polymers were soluble in CH_2Cl_2, $CHCl_3$, 1,4-dioxane, and so forth before irradiation, not one of the polymers was soluble in any solvent. All the experimental data indicate that photo
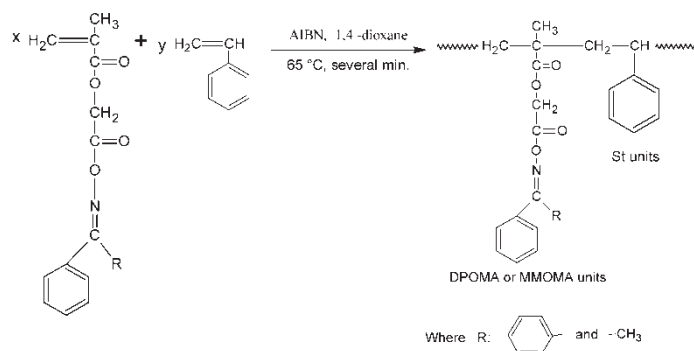
Sch. 3. Synthesis of the copolymers.

degradation in the oxime ester region occurred and cross-linking followed. A photo degradation mechanism of the oxime esters are shown in Scheme 4. Dissociation of oxime leads to iminyl radical and acyloxyl radical (RCO_2). If the decarboxylation is not fast enough, these two radicals can be recombined to give the starting oxime, and therefore the global efficiency of the photodissociation is decreased (36). On the contrary, the occurrence of the decarboxylation process leads to the formation of carbon dioxide and a new radical (R). The latter can also react in-cage with the iminyl radical to form an imine, resulting, in a decrease of the free iminyl radical quantum yield. Similar results were obtained for the DPOMA-St and MMOMA-St copolymers. The polymers react photochemically according to a mechanism similar to that found for *O*-acyloximes and its derivatives (17). Though practical evaluation from spectral data is rather dubious because sensitivity of photocrosslinkable polymers is a

function of Tg, molecular weight, polymer solubility etc., the discrimination of photoresponsibilities of chromophores themselves is possible to a certain extent.

3.4 Molecular Weights of Polymers

The number average ($\bar{M}_n$) and weight average ($\bar{M}_w$) molecular weights and the polydispersty index of homopolymers as well as copolymer samples were determined by GPC with polystyrene and tetrahydrofuran as the standard and solvent, respectively, and given in Table 1. The PDIs of the polymers range between 1.63−1.88. The theoretical values of PDI for polymers via radical recombination and disproportionation are 1.5−2.0, respectively (37). In the free radical polymerization of methacrylate monomers, the polymeric radicals undergo termination mainly by disproportionation (38). Hence, the polydispersity index value of polymers suggests a greater tendency for chain termination by disproportionation than radical recombination, which is the case with many methacrylates.

3.5 Thermal Analysis

The thermal stabilities of the polymers were investigated by thermogravimetric analysis (TGA) in a nitrogen stream at a heating rate of 20°C min^{-1}. Thermogravimetric curves of the copolymers are compared with those of the homopolymers in Figure 8. The initial decomposition temperatures of poly (DPOMA) and poly (MMOMA) are around 200 and 170°C, respectively and independent of the side-chain structures. This result shows that main-chain scission is an important reaction in the degradation of polymers, at least in the
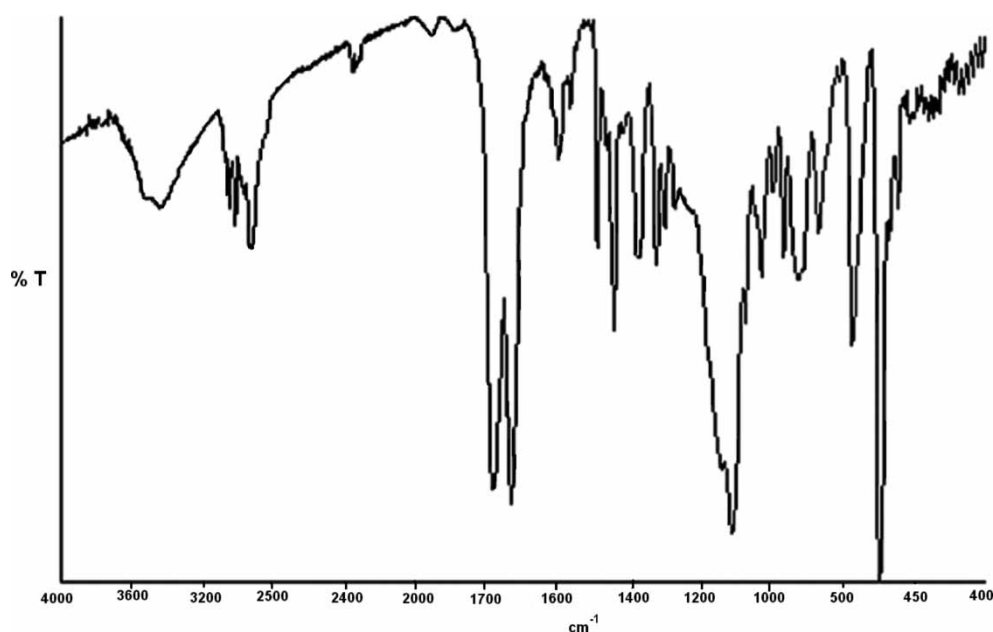

Fig. 4. FT-IR spectrum of poly(DPOMA-co-St) (DPOMA: 52.6 by molar percentage).
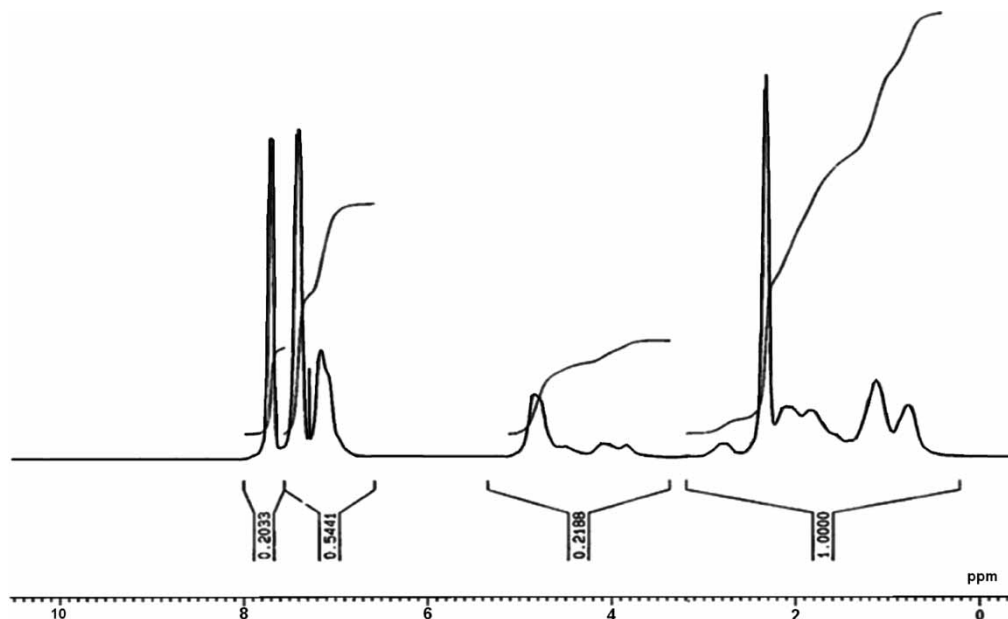
Fig. 5. ¹H-NMR spectrum of poly(MMOMA-co-St) (MMOMA: 52.2 by molar percentage).

beginning. The degradation of poly (DPOMA) occurred in three stages. The first stage was observed 195–300°C. The second stage decomposition commenced at 310–395°C, and the last stage was observed 405–500°C. Poly (MMOMA) undergoes three stages decomposition. The first stage was observed at 170–275°C. The second stage decomposition commenced at 295–375°C, and the last stage was observed at 390–500°C. The residue at 450°C for the both polymers is about 10%. Poly (St) was stable to heat up to 500°C, and maximum degradation (75%) occurs at 500°C. The thermal stability of the copolymers was improved by the incorporation of St. The initial decomposition temperatures of the copolymers were between those of the homopolymers. The data are presented in Table 2.

3.6 Activation Energy of the Ccopolymers

The activation energies on the thermal decomposition of copolymers were determined by thermogravimetric analysis. Isothermal thermogravimetry is superior to obtain accurate activation energy for thermal degradation, although it is time-consuming. In the case of thermal degradation of polymers, in which depolymerization is competing with cyclization or crosslinking due to side groups, the TG at various heating rates is much more convenient than ITG for the investigation of thermal degradation kinetics. The activation energy of the decomposition process was determined by multiple heating rate kinetics (MHRK) (39) method. The typical procedure for the calculation of activation energy for copolymers was as follows: thus, the series of experiments were run at different heating rates, ΔE_a could be obtained from the slope of a linear plot of

log (heating rate) vs. $1/T$. Figure 9 shows the normalized weight loss vs. temperature for poly(MMOMA) at different heating rates. The activation energies of degradation calculated from TGA curves are based on weight loss at different decompositions regions during degradation. The calculation of activation energies of the others copolymers were done by the same measurements. From the slopes, we calculate the average activation energies for the thermal degradation of copolymers are reported in Table 3. It is shown that this result was similar to methacrylate polymers in the literature (40, 41).
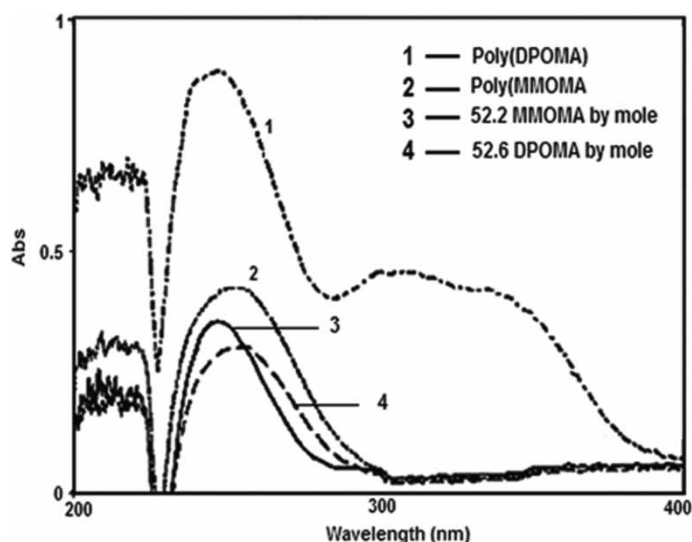

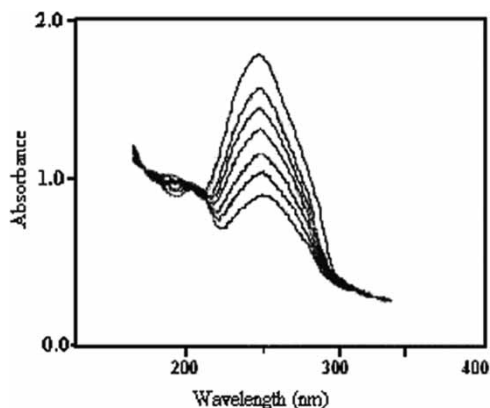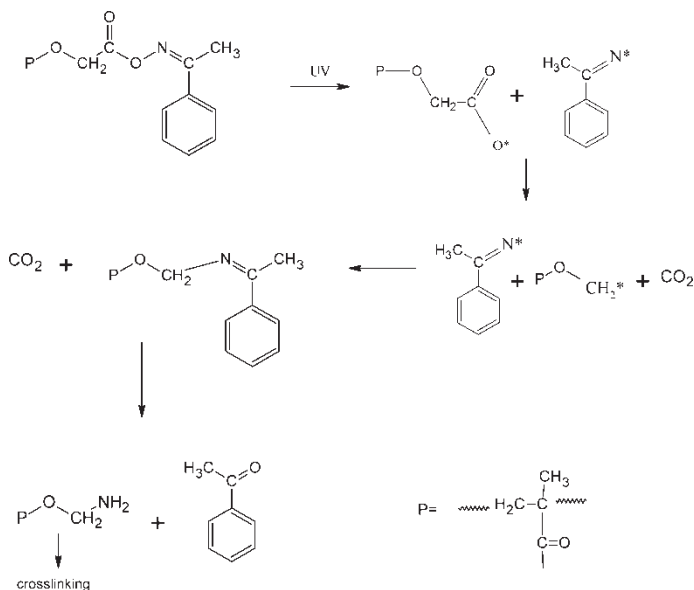**Fig. 6.** Absorption spectra of the polymers in the film state.

Fig. 7. UV sprectral changes due to the photoreaction of poly (MMOMA) in the film state (0,10,20,40,80,140, and ∞).

Fig. 8. Thermograms of homopolymers and various copolymers.

3.7 Determination of Monomer Reactivity Ratios

Copolymerization of DPOMA and MMOMA with St in 1, 4-dioxane solution was studied for a molar fraction of St from approximately 0.90 to 0.20 in the feed. The amounts of monomeric units in the copolymers were determined by elemental analysis. The monomer reactivity ratios for the copolymerization of St with DPOMA and MMOMA were determined from the monomer feed ratios and the copolymer composition. The Fineman-Ross (FR) and Kelen-Tüdös (KT) methods were used to determine the monomer reactivity ratios. The significance of parameters of FR and KT equations are presented in Table 4. According to the FR method the monomer reactivity ratios can be obtained by the equation:

$$G = Hr_1 - r_2 \tag{1}$$

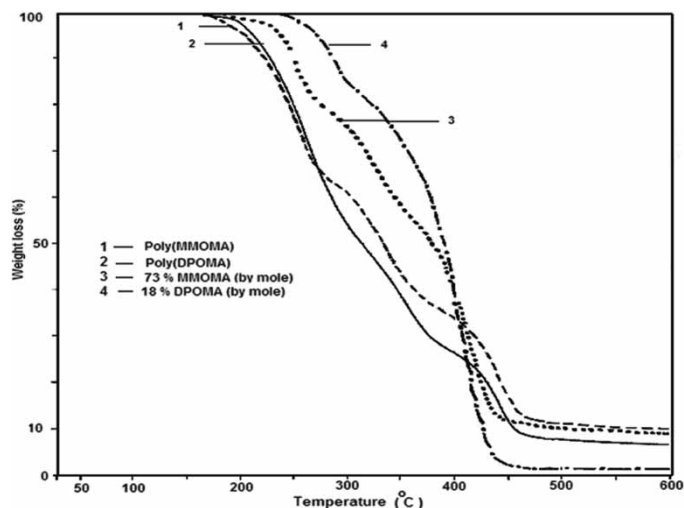**Sch. 4.** Photo degradation mechanism of the polymers.

where the reactivity ratios, r_1 correspond to the DPOMA, MMOMA, and r_2 correspond to the St monomers. The parameters G and H are defined as follows:

$$G = \frac{F(f-1)}{f} \quad \text{and} \quad H = \frac{F^2}{f} \tag{2}$$

with

$$F = \frac{M_1}{M_2} \quad \text{and} \quad f = \frac{m_1}{m_2} \tag{3}$$

M_1 and M_2 are the monomer molar compositions in feed and m_1 and m_2 the copolymer molar compositions. Alternatively, the reactivity ratios can be obtained using the KT method which is based on the equation:

$$\eta = \left(r_1 + \frac{r_2}{\alpha}\right)\xi - \frac{r_2}{\alpha} \tag{4}$$

Where η and ξ are functions of the parameters G and H:

$$\eta = \frac{G}{\alpha + H} \quad \text{and} \quad \xi = \frac{H}{\alpha + H} \tag{5}$$

and α a constant which is equal to $(H_{max} \cdot H_{min})^{1/2}$, H_{max}, H_{min} being the maximum and the minimum H values, respectively from the series of measurements. From the linear plot of η as a function of ξ the values of η for $\xi = 0$ and $\eta = 1$ is used to calculate the reactivity ratios according to the equations:

$$\xi = 0 \implies \eta = -r_1/\alpha \text{ and } \xi = 1 \implies \eta = r_2 \tag{6}$$

The graphical plots concerning the methods previously reported are given in Figures 10, 11; whereas the reactivity ratios are summarized in Table 5.

In all cases, and for all graphical methods, the plots were linear indicating that these copolymerizations follow the conventional copolymerization kinetics and that the reactivity of a polymer radical is determined only by the terminal

Table 2. Selected TGA results for homopolymers and copolymers

Polymer	IDT ($^{\circ}$C)[a]	The temperature ($^{\circ}$C) for a weight loss			The resiude (%) at 450°C
		20	50	70	
Poly(St)	325	380	400	450	2
Poly(MMOMA-co-St)					
(21/79)	300	416	400	382	5
(52/48)	285	420	384	347	11
(72/28)	175	430	382	318	13
Poly(MMOMA)	170	440	328	260	6
Poly(DPOMA-co-St)					
(18/82)	315	415	388	354	3
(52/48)	305	405	347	297	6
(74/26)	220	410	322	282	9
Poly(DPOMA)	195	428	313	265	12

[a]Initial decomposition temperature.

monomer unit. For DPOMA and St systems, the r_1 values are higher than the r_2 values. The higher r_1 value of DPOMA confirms the higher reactivity of DPOMA compared with that of St. For MMOMA and St systems the r_1 values are higher than the r_2 values. The higher r_1 value of MMOMA confirms the higher reactivity of MMOMA compared with that of St. Although the reactivities of growing radicals with the DPOMA and MMOMA ends are higher toward St than DPOMA and MMOMA, the reactivity of growing radicals with the St end is higher toward DPOMA and MMOMA than St. The reactivity ratio values (r_1 and r_2) of poly(DPOMA-co-St) and poly(MMOMA-co-St) are less than one. The product $r_1 \cdot r_2$ indicates that the two system copolymerize randomly in the polymer chain although there is a possible tendency for alternation.

3.8 Glass Transition Temperatures

The glass transition (T_g) temperatures were determined using a Perkin-Elmer Pyris1 DSC. Samples of about 5–8 mg held in sealed aluminum crucibles and the heating rate of 20°C/min under a dynamic nitrogen flow were used for the measurements. From DSC measurements T_g was taken as the

Fig. 9. Normalized weight loss vs. temperature for the thermal degradation of poly(MMOMA-co-St) (MMOMA: 72.3 by molar percentage).

Table 3. Thermal decomposition data and activation energies of the polymers

Sample	Stage of decomposition	Temperature range ($^{\circ}$C)	Average activation energy (kJ/mol)	T_g
Poly(DPOMA)	Stage 1	195–30049[a]	95.65	59
	Stage 2	310–395(23)	83.40	
	Stage 3	405–500(19)	71.50	
Poly(DPOMA-co-St)				
(18/82)	Single	250–450(3)	97.60	104
(52/48)	Single	210–500(5)	89.40	91
(74/26)	Single	200–500(8)	83.70	61
Poly(MMOMA)	Stage 1	170–275(35)	89.70	57
	Stage 2	295–375(27)	93.50	
	Stage 3	390–500(11)	97.70	
Poly(MMOMA-co-St)				
(21/79)	Single	255–500(4)	103.40	102
(52/48)	Single	245–50(11)	97.70	95
(72/28)	Single	210–500(10.6)	88.30	62

[a]Figures in parenthesis indicate weight loss (%) during to temperature range stated.
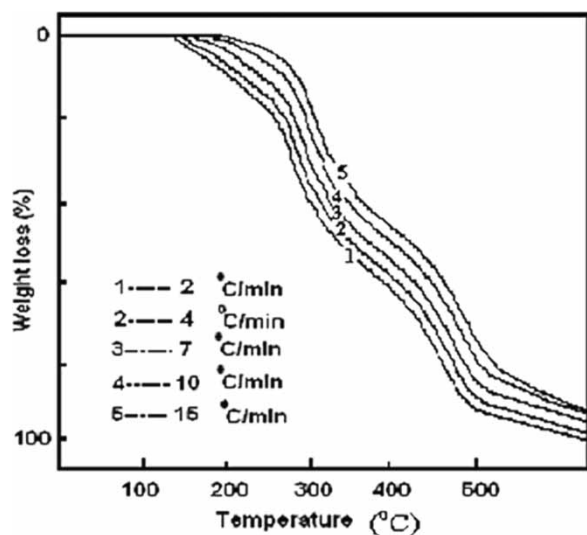
Table 4. FR and KT parameters for copoly(MMOMA-St) and copoly(DPOMA-St) system

System	$F = M_1/M_2$	$f = m_1/m_2$	$G = F(f-1)/f$	$H = F^2/f$	$\mu = G/\alpha + H$	$\zeta = H/\alpha + H$
Poly(MMOMA-co-St)						
1	0.111	0.267	−0.305	0.046	−0.528	0.079
2	0.250	0.458	−0.296	0.136	−0.444	0.204
3	0.538	0.838	−0.104	0.345	−0.119	0.394
4	1.000	1.090	0.083	0.917	0.057	0.633
5	1.857	1.469	0.593	2.347	0.206	0.815
6	4.000	2.610	2.467	6.130	0.370	0.920
Poly(DPOMA-co-St)						
1	0.111	0.217	−0.401	0.057	−0.645	0.092
2	0.250	0.446	−0.311	0.140	−0.442	0.199
3	0.538	0.695	−0.236	0.416	−0.241	0.424
4	1.000	1.109	0.098	0.902	0.067	0.615
5	1.857	1.217	0.331	2.834	0.097	0.834
6	4.000	2.872	2.607	5.571	0.425	0.908

$\alpha = 0.531$ for the poly(MMOMA-co-St) system and $\alpha = 0.563$ for the poly(DPOMA-co-St) system.

midpoint of the transition region. A plot of copolymer composition vs, glass-transition temperatures of the copolymers is shown in Figure 12. The T_g of poly (St) is 105°C, and that of poly (DPOMA) is 59°C and poly (MMOMA) is 57°C, respectively. In comparison to that of poly (DPOMA) or poly (MMOMA), the shift to higher temperature is also noted for all the copolymers studied and their magnitudes are dependent on the increasing in St molar fraction in the copolymer chain. An increase in T_g of copolymers may be due to the introduction of comonomer into poly (DPOMA) or poly (MMOMA), St, which increases the inter-molecular polar interactions between the molecular chains due to structure stretching. The data are presented in Table 3. The results clearly indicate that T_g values of copolymers depend on the composition of comonomers and increase with increasing St content in the polymer chain. It can be seen that the observed T_g increases with decreasing DPOMA or MMOMA and presents a striking positive deviation with respect to linearity, which can be associated with a lower free volume, mobility and flexibility than a mixture of DPOMA or MMOMA and St units.

3.9 Antibacterial and Antifungal Effects of the Monomers and Polymers

The biological activities of the monomers and their homopolymers and copolymers were tested against different microorganisms with DMSO as the solvent. The sample concentrations were 100 µg. All microorganism strains were obtained from the Culture Collection of Microbiology Laboratory of Afyon Kocatepe University (Afyon, Turkey).

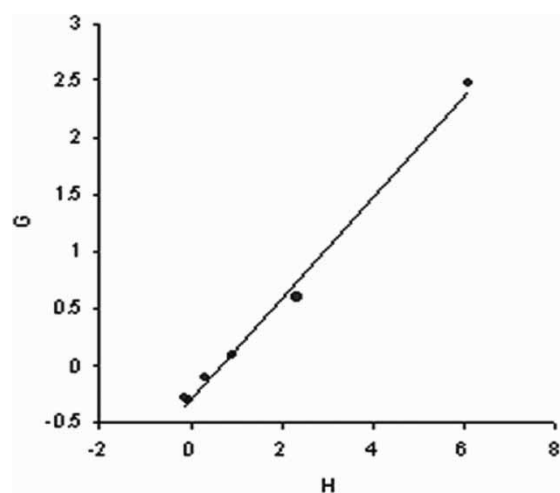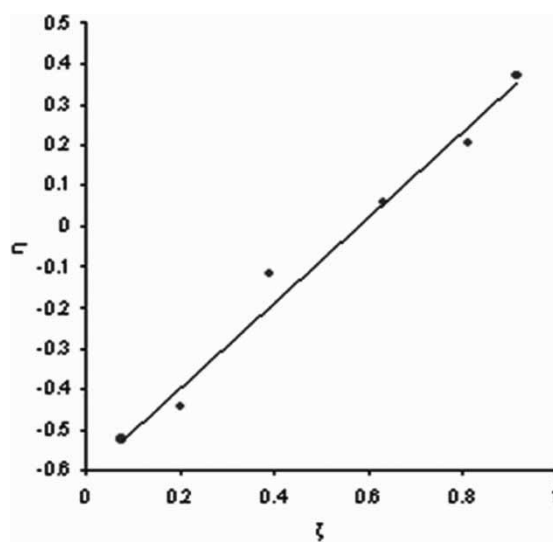**Fig. 10.** FR plot for the determination of reactivity ratios of the MMOMA-St copolymer system.

Fig. 11. KT plot for the determination of reactivity ratios of the MMOMA-St copolymer system.

Table 5. Comparison of reactivity ratios by various methods

System	Methods	r_1	r_2	r_1r_2	$1/r_1$	$1/r_2$
Poly(MMOMA-co-St)	FR	0.44 ± 019	0.30 ± 0.14	0.12	2.26	3.37
	KT	0.44 ± 0.17	0.32 ± 0.15	0.14	2.26	3.09
	Average	0.44 ± 0.15	0.31 ± 0.22	0.13	2.26	3.23
Poly(DPOMA-co-St)	FR	0.50 ± 0.21	0.48 ± 0.18	0.24	1.98	2.06
	KT	0.44 ± 0.16	0.40 ± 0.17	0.18	2.28	2.50
	Average	0.47 ± 0.19	0.44 ± 0.2	0.22	2.13	2.28
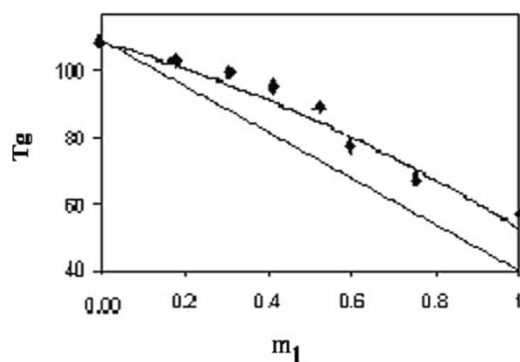
Fig. 12. Dependence of the glass transition temperature on the mol fraction of MMOMA in poly(MMOMA-co-St), by DSC.

In this study, *Staphylococcus aureus* ATCC 29213, *Escherichia coli* ATCC 25922 and *Pseudomonas aeruginosa* ATCC 27853 were used as bacteria. *Candida albicans* CCM 31 was a fungus. YEPD medium cell culture was prepared as described by Connerton (42). Ten milliliters of YEPD medium were inoculated with each cell from plate cultures. Yeast extract 1% (w/v), bactopeptone 2% (w/v), and glucose 2% (w/v), was obtained from Difco. Microorganisms were incubated at 35°C for 24 h. About 1.5 ml of these overnight stationary phase cultures were inoculated onto 250 ml of YEPD and incubated at 35°C until OD_{600} reached 0.5.

The antibiotic sensitivity of the polymers was tested with the antibiotic disk assay as described (43). Nutrient Agar (NA) was purchased from Merck. About 1.5 ml of each prepared different cell culture were transferred into 20 ml of NA and mixed gently. The mixture was inoculated into the plate. The plates were rotated firmly and allowed to dry at room temperature for 10 min. Prepared antibiotic discs (100 µg) were placed on the surface of the agar medium (44). The plates were kept at 5°C for 30 min and then incubated at 35°C for 2 days. If a toxic compound leached out from the disc, it means that the microbial growth is inhibited around the sample. The width of this area expressed the antibacterial or antifungal activity by diffusion. The zones of inhibition of microorganism growth of the

Table 6. Antimicrobial effects of the compounds (mm of zones)

Compounds	*Pseudomonas aeruginosa*	*Escherichia coli*	*Candida albicans*	*Staphylococcus aureus*
MMOMA	—	—	8	15
DPOMA	7	10	8	—
Poly(MMOMA)	—	11	—	—
Poly(DPOMA)	—	10	—	9
Poly(MMOMA-co-St)				
(21/79)	9	—	—	—
(52/48)	7	22	—	—
(72/28)	10	—	—	—
Poly(DPOMA-co-St)				
(18/82)	7	12	—	—
(52/48)	—	10	13	11
(74/26)	—	9	10	—
Moxiploxacin	15	—	—	35
Penicilin G	—	6	—	35
Levofloxacin	20	—	9	30
Amikacin	20	6	18	20
Ciprolfoxacin	15	6	—	30
Teicoplanin	—	6	12	15
DMSO	—	—	—	—

Compound concentration: 100 µg/disc; the symbol (—) reveals that the compounds have any activity against the microorganism.
DMSO: Dimethylsulfoxide (control).

standard samples monomers, homopolymers and copolymers, were measured with a millimeter ruler at the end of the incubation period. It has been suggested that the monomers and their copolymers with N and O donor system and carboxyl and oxime esters groups might have inhibition on the enzyme production, which that require a free hydroxy group for their activity appear to be especially susceptible to deactivation by the donor atoms of the polymers. The results were compared with the standard drugs as moxiploxacin, penicilin, g. levofloxacin, amikacin, ciprolfoxacin, teicoplanin. The results suggest that the monomers, polymers and the some copolymers have good biological activity on the *Escherichia coli* microorganisms in comparison with standard drugs. However, monomers and polymers exhibiting and inhibition zone significantly increased with antibiotic discs of the polymer in the culture, depending on the disc concentration. The data are listed in Table 6 and are the average data of two experiments.

4   Conclusions

The synthesis of new methacrylate monomers having pendant oxime ester moieties have been reported for the first time. The structure of both monomer and their polymers were characterized by spectroscopic methods. Copolymers of these monomers with St having different copolymer compositions were prepared. The reactivity ratio values have been discussed. The reactivity ratio values were derived from the F-R and K-T methods were in good agreement with each other. The higher r_1 value of DPOMA or MMOMA confirms the higher reactivity of DPOMA or MMOMA with that of St, and the copolymer sequence will be statistical in structure with more DPOMA or MMOMA. The biological activity and thermal stability of the polymers were investigated. The monomers and polymers had good biological activity in comparison with standard drugs. The decomposition activation energies of the polymers were calculated with the MHRK method. The molecular weights of the polymers were determined by GPC. Finally, the photocrosslinking behavior of the polymers as thin films was tested in the presence of UV light. The increasing utility of photosensitive polymers in many applications, such as microelectronics, printing and UV-curable lacquers, and inks, has provided us with an incentive to obtain novel polymers.

5   Acknowledgements

6   References

1. Parker, S. and Braden, M. (1989) *Biomaterials*, **10**, 91.
2. Nicholson, J.W., Brookman, P.J., Lacy, O.M., Sayers, G.S. and Wilson, A.D. (1998) *J. Biomed. Mater. Res.*, **22**, 623.
3. Erol, I. (2004) *J. Polym. Sci. Part A: Polym. Chem.*, **42**, 3157.
4. Soykan, C., Erol, I. and Kirbag, S. (2003) *J. App. Polym. Sci.*, **90**, 3244.
5. Simms, J.A. (1961) *J. App. Polym. Sci.*, **5**, 58.
6. Ghogare, A. and Kumar S. (1989) *J. Chem. Soc., Chem. Com.*, **1533**, 5.
7. Ghogare, A. and Kumar, S. (1989) *J. Chem. Soc., Chem. Com.*, **134**, 5.
8. Moris, F. and Gotor, V. (1993) *J. Org. Chem.*, **58**, 653.
9. Athawale, V. and Manjrekar, N. (2000) *J. Mol. Catal. B: Enzymatic*, **10**, 551.
10. Athawale, V., Manjrekar, N. and Athawale, M. (2001) *J. Mol. Catal. B Enzymatic*, **16**, 169.
11. Athawale, V., Manjrekar, N. and Athawale, M. (2002) *Tetrahedron Lett.*, **43**, 4797.
12. Shirai, M. and Tsunooka, M. (1998) *Bull. Chem. Soc. Jpn.*, **71**, 2483.
13. Shirai, M., Nakanishi, J., Tsunooka, M., Matsuo, T. and Endo, M. (1998) *J. Photopolym. Sci. Technol.*, **11**, 641.
14. Song, K.H., Tsunooka, M. and Tanaka, M. (1998) *J. Photochem. Photobiol. A: Chem.*, **44**, 197.
15. Tsunooka, M., Tachi, H., Asakino, K. and Suyama, K. (1999) *J. Photosci.*, **6**, 145.
16. Chae, K.H. (1998) *Macromol. Rapid Commun.*, **19**, 1.
17. Shirai, M., Endo, M. and Tsunooka, M. (1999) *J. Photopolym. Sci. Technol.*, **12**, 669.
18. Lalevee, J., Allonas, X., Fouassier, J.P., Tachi, H., İzumitani, A., Shirai, M. and Tsunooka, M. (2002) *J. Photochem. Photobiol. A: Chem.*, **151**, 27.
19. Theodorakis, E.A. and Wilcoxen, K.M. (1996) *Chem. Commun.*, 1927.
20. Hwu, J.R., Tsay, C.S., Hong, S.C., Leu, Y.J., Liu, C.F. and Chou, S.S.P. (2003) *Tetrahedron Lett.*, **44**, 2957.
21. Moeller, N., Kangarloo, B.S., Puscasu, I., Mock, C., Krebs, B. and Wolff, J.E.A. (2000) *Anticancer Res.*, **20(6B)**, 4435.
22. Polson, S.M., Cini, R., Pifferi, C. and Marzilli, L.G. (1997) *Inorg. Chem.*, **36(15)**, 3390.
23. Dreos, R., Tauzher, G., Trendafilova, D.H., Nardin, G. and Randaccio, L. (1996) *Inorg. Chem.*, **35(10)**, 2715.
24. Su, S., Acquilano, D.E., Arumugasamy, J., Beeler, A.B., Eastwood, E.L., Giguere, J.R., Lan, P., Lei, X., Min, G.K., Yeager, A.R., Zhou, Y., Panek, J.S., Snyder, J.K., Schaus, S.E. and Porco, J.A. (2005) *J. Org. Lett.*, **7(13)**, 2751.
25. Kaneko, K., Uchida, T., Shibuya, S., Honda, T., Kawamoto, I., Harasaki, T., Fukuoka, T. and Konusu, T. (2002) *Bioorg. Med. Chem. Lett.*, **12**, 803.
26. Arshady, R., Kenner, G.W. and Ledwith, A. (1981) *Macromol. Chem. Phys.*, **182(1)**, 41.
27. Ham, G. *Copolymerization High Polymers*; Interscience: New York, Vol. 18, 1964.
28. Fineman, M. and Ross, S.D. (1950) *J. Polym. Sci.*, **5**, 259.
29. Kelen, T. and Tudos, F. (1975) *J. Macromol. Sci. Chem.*, **A9**, 1.
30. Kelen, T., Tudos, F., Turesanyi, B. and Kennedy, M. (1977) *J. Polym. Sci. Part A: Polym. Chem.*, **15**, 3041.
31. Ozawa, T. (1965) *Bull. Chem. Soc. Japan.*, **38**, 1881.
32. Nishada, H., Yamashita, M. and Endo, T. (2002) *Polym. Degrad. Stab.*, **78**, 129.
33. Vogel, A. *Vogels Textbook of Practical Organic Chemistry*; Longman, Vol. 813, 1989.
34. Erol, I. and Soykan, C. (2003) *React. Funct. Polym.*, **56**, 147.
35. Yoshida, M., Sakuragi, H., Nishimura, T., Ishikawa, S.I. and Tokumaru, K. (1975) *Tetrahedron Lett.*, 1125.

36. McCarroll, A.J. and Walton, J.C. (2000) *J. Chem. Soc. Perkin Trans.*, **2**, 2399.

37. Teramachi, S., Hasegawa, A., Akatsuka, M., Yamashita, A. and Takemoto, N. (1978) *Macromolecules*, **11**, 1206.

38. Bevington, J.C., Melville, H.W. and Taylor, R.P. (1954) *J. Polym. Sci.*, **12**, 449.

39. Flynn, J.H. and Wall, L.A. (1966) *Polym. Lett.*, **4**, 323.

40. Ho, B.C., Lee, Y.D. and Chin, W.K. (1992) *J. Polym. Sci. Part A: Polym. Chem.*, **30**, 2389.

41. Coşkun, M., Demirelli, K., Erol, I. and Ahmedzade, M. (1998) *Polym. Deg. Stab.*, **61**, 493.

42. Connerton, I.F. In *Analysis of Membrane Proteins*; Gould, G.W. (ed.); Portland: London. 177, 1994.

43. Chan, E.C.Z., Pelczar, M.J. and Krieg, N.R. Agar diffusion method. In *Laboratory Exercises in Microbiology*; Chan et al. (ed.); Mc-Graw-Hill: New York, 225, 1993.

44. Desai, J.A. (1996) *J. Macromol. Sci., Pure and Appl. Chem.*, **33**, 1113.